applied sciences

MDPI

Article

A Layer-Based CAD-to-FEM Workflow for Seismic Assessment of Existing Reinforced Concrete Bridges

Marco Zucca [1,*], Elisa Pilia [1] and Pietro Crespi [2]

1 Department of Civil and Environmental Engineering and Architecture, University of Cagliari, Via Marengo 2, 09123 Cagliari, Italy; elisa.pilia@unica.it
2 Department of Architecture, Built Environment and Construction Engineering, Politecnico di Milano, Piazza Leonardo da Vinci 33, 20133 Milan, Italy; pietro.crespi@polimi.it
* Correspondence: marco.zucca2@unica.it

Abstract

The numerical modelling of existing reinforced concrete (RC) bridges represents one of the most time-consuming and operator-dependent phases of seismic vulnerability assessment. Although advanced nonlinear analysis procedures are widely available, the generation of finite element (FE) models is still commonly performed through manual operations, limiting modelling efficiency, repeatability, and interoperability between design and analysis environments. This paper presents a layer-based CAD-to-FEM workflow for the structured generation of simplified FE models of existing RC bridges. The proposed methodology uses a standardized layer-based CAD organization and direct DXF interoperability with MIDAS Civil to transfer a centroidal representation of the bridge into a simplified beam-based finite element model. The centroidal axes of the bridge components are extracted from the original engineering drawings and classified into dedicated structural layers, providing a structured basis for subsequent FE model generation. The proposed workflow is designed to reduce manual preprocessing operations and improve modelling consistency by organizing the structural geometry through standardized CAD layers, thereby facilitating the generation of analysis-ready models for seismic assessment. The workflow is integrated with a Multi-Modal Pushover Analysis (MPA) procedure to evaluate the seismic vulnerability of bridges characterized by multiple significant vibration modes. A case study involving an existing Italian RC bridge demonstrates the feasibility of using the proposed simplified modelling strategy within a multi-modal nonlinear seismic assessment, including the evaluation of both ductile and brittle collapse mechanisms through seismic risk indices. The proposed workflow provides a structured framework for integrating conventional engineering drawings with nonlinear seismic assessment procedures.

Keywords: CAD-to-FEM; RC bridges; seismic assessment

Check for updates

Academic Editor: Sang-Hyo Kim

Received: 6 August 2026
Revised: 19 August 2026
Accepted: 31 August 2026
Published: 2 September 2026

1. Introduction

The assessment of the seismic vulnerability of existing reinforced concrete (RC) bridges has become a priority for infrastructure owners and road authorities worldwide, particularly for structures designed before the introduction of modern seismic provisions [1–5]. A significant portion of the existing bridge stock was constructed between the 1960s and 1970s and is characterized by inadequate seismic detailing, material degradation, and increasing maintenance demands [6]. Consequently, reliable numerical procedures capable of rapidly evaluating the structural performance of these infrastructures have become essential for supporting maintenance planning and risk mitigation strategies.

Several methodologies have been developed for the seismic assessment of existing bridges, differing considerably in terms of accuracy, computational demand and applicability to large structural inventories. Conventional nonlinear static procedures provide an effective compromise between computational efficiency and the ability to represent structural nonlinearities, but their accuracy may decrease when higher-mode effects significantly influence the seismic response. Multi-modal pushover procedures address this limitation by explicitly accounting for the contribution of several vibration modes and are therefore particularly suitable for long or irregular bridge structures [7]. Nonlinear time-history analyses provide a more detailed representation of the structural response and allow the effects of ground-motion characteristics and nonlinear response evolution to be explicitly considered. However, their application requires the selection and processing of appropriate seismic records and a substantially greater computational effort, particularly when several structures or seismic scenarios must be investigated [8].

Fragility-based approaches provide a different perspective by expressing structural vulnerability in probabilistic terms and are particularly useful for risk assessment at network level. Their reliability, however, depends on the availability of representative structural models, appropriate ground-motion sets and a sufficiently large number of nonlinear analyses. Incremental Dynamic Analysis further extends nonlinear dynamic assessment by evaluating structural response over progressively increasing levels of seismic intensity, providing detailed information on the evolution from elastic response to collapse. The associated computational cost can nevertheless become significant when applied systematically to large bridge inventories [9]. Therefore, while increasingly sophisticated analysis methods can improve the characterization of seismic response, their practical implementation remains strongly dependent on the availability of reliable and efficiently generated numerical models.

In parallel with developments in structural analysis, considerable research has focused on the digital representation of existing bridges and on interoperability between geometric and information models and structural-analysis environments. CAD-to-FEM and BIM-to-FEM approaches facilitate the transfer of geometric and structural information to finite element environments, reducing repeated model reconstruction and supporting more consistent model development. In bridge applications, Bridge Information Modelling (BrIM) extends this concept by organizing geometry, structural components, inspection data and asset information within bridge-specific digital representations. More recent developments have increasingly focused on automated model generation. Scan-to-BIM and Scan-to-BrIM procedures exploit laser scanning, photogrammetry and point-cloud data to reconstruct bridge geometry and identify structural components, while other approaches aim at generating analysis-oriented models directly from digital survey information. Digital-twin frameworks further integrate geometric models, finite element representations, monitoring data and model-updating procedures, providing continuously evolving digital representations of physical infrastructure. These approaches represent important advances toward increasingly automated and information-rich bridge modelling. Despite these developments, their objectives and input requirements differ from those considered in the present study. Advanced BIM/BrIM, Scan-to-BIM and digital-twin frameworks generally rely on detailed information models, point clouds, monitoring data or dedicated recognition algorithms. Conversely, a substantial portion of the existing bridge stock is still documented primarily through conventional engineering drawings. For global seismic assessment based on simplified FE models, reconstructing a high-fidelity information model may not always be necessary. A complementary need therefore exists for lightweight procedures capable of translating conventional engineering drawings into structurally organized, analysis-ready representations while limiting intermediate modelling operations. From this perspective, the main challenge is not exclusively to increase the sophistication of the structural analysis, but also to establish efficient and repeatable procedures connecting existing geometric information with analysis-ready numerical models. Existing digital modelling approaches generally emphasize either detailed geometric reconstruction and information management or advanced structural analysis, whereas the intermediate step required to translate conventional bridge drawings into simplified structural models remains comparatively less standardized. A practical gap therefore exists between the availability of engineering drawings and digital geometric data, on the one hand, and the efficient generation of consistent finite element models suitable for nonlinear seismic assessment, on the other. Within this context, CAD-to-FEM interoperability and DXF-based geometry transfer are not considered novel contributions of the present study. The specific contribution lies in the definition of a lightweight, analysis-oriented workflow tailored to existing RC bridges for which conventional engineering drawings represent the primary source of geometric information. The procedure combines a standardized centroidal representation with a predefined functional layer structure that preserves the topology and connectivity required for the generation of a simplified beam-based FE model. Unlike high-fidelity BIM/BrIM and Scan-to-BIM approaches, the proposed workflow intentionally retains only the geometric and structural information required for global seismic assessment. The resulting model is then directly integrated into a nonlinear Multi-Modal Pushover Analysis framework accounting for both ductile and brittle failure mechanisms. The contribution should therefore be understood as the standardization and integration of the drawing-to-analysis process rather than as a new CAD-to-FEM interoperability technology.

To overcome these limitations, this study proposes a layer-based CAD-to-FEM workflow specifically developed for existing RC bridges. The methodology starts from conventional AutoCAD drawings in which the structural members are represented by centroidal axes rather than external geometries. The bridge components, including deck, piers and bearings, are organized into dedicated CAD layers that can be directly imported into MIDAS Civil by means of DXF files. This approach enables the structured generation of simplified beam-based finite element models while retaining the global structural characteristics required for seismic analysis. The layer-based organization is intended to standardize the transfer of structural information between the CAD and FE environments and to reduce user-dependent operations during model implementation.

The proposed workflow is intended for global bridge assessment, where simplified beam-based numerical models provide an effective compromise between modelling efficiency and computational accuracy. By standardizing the transition from engineering drawings to finite element models, the methodology provides a structured framework that may support the systematic assessment of bridge inventories.

Once generated through the proposed workflow, the finite element model is employed for seismic vulnerability assessment using the Multi-Modal Pushover Analysis (MPA). Unlike conventional pushover procedures, which may provide inaccurate results for structures exhibiting several significant vibration modes, the MPA considers the contribution of multiple modal responses and is therefore particularly suitable for long and irregular bridge systems [10,11]. The nonlinear behaviour of reinforced concrete members is represented through concentrated plastic hinges, allowing accurate simulation of both ductile and brittle collapse mechanisms while maintaining limited computational effort.

It should be clarified that the MPA procedure itself is not a methodological contribution of the present study. Rather, it is adopted as an established nonlinear assessment framework to demonstrate the usability of the FE model generated through the proposed CAD-to-FEM workflow.

https://doi.org/10.3390/app16178723

The proposed methodology is demonstrated through a proof-of-concept application to an existing RC bridge located in Northern Italy. The case study illustrates the implementation of the layer-based CAD-to-FEM workflow and its integration with nonlinear Multi-Modal Pushover Analysis. The application demonstrates the feasibility of generating an analysis-ready simplified model from a structured CAD representation and subsequently using it for the evaluation of both ductile and brittle seismic failure mechanisms. Quantitative validation of modelling accuracy, efficiency and repeatability against independently developed reference FE models remains a necessary step for future research.

The remainder of the paper is organized as follows. Section 2 describes the proposed CAD-to-FEM workflow and the nonlinear modelling strategy. Section 3 presents its application to an existing reinforced concrete bridge, while Sections 4 and 5 discuss the obtained results and summarize the main conclusions.

2. Methodology

2.1. Layer-Based CAD-to-FEM Workflow

The proposed methodology is based on a standardized CAD-to-FEM workflow developed to support the structured generation of finite element models of existing reinforced concrete bridges and the systematic transfer of geometric information from engineering drawings to the numerical model.

The workflow starts from the original engineering drawings available in AutoCAD format [12]. Instead of reproducing the external geometry of every structural member, the bridge is transformed into a centroidal representation in which each component is described by its geometric axis. This simplification is based on the observation that global seismic analyses mainly depend on the stiffness, mass distribution and structural connectivity of the bridge rather than on the detailed geometry of individual components. Consequently, representing the bridge through centroidal beam axes considerably reduces the complexity of the numerical model while preserving the structural characteristics governing its dynamic response. At the present stage, the generation of the centroidal representation is performed manually by the analyst within the CAD environment. The proposed workflow should therefore be regarded as semi-automatic. Automation is introduced in the subsequent model-transfer stage, where the predefined layer organization enables structural components to be systematically recognized and associated with the corresponding finite element typologies during DXF import. Accordingly, the present study focuses on reducing and standardizing the manual operations required for model transfer and implementation rather than on providing a fully automatic drawing-to-FE conversion. Accordingly, two different levels of operator involvement can be distinguished within the workflow. The interpretation of the original engineering drawings, identification of the structural members, extraction of their centroidal axes, and definition of the structural idealization remain analyst-dependent steps requiring engineering judgement. Once this representation has been established, the subsequent organization of the structural entities into predefined functional layers and their transfer through the DXF interface follow a standardized procedure. Layer naming, element categorization and the association between CAD entities and the corresponding FE typologies are predefined within the workflow, whereas section properties, support conditions and modelling assumptions must still be assigned according to the available structural information and the adopted assessment model. Therefore, the present workflow standardizes the model-transfer and organization stages but does not eliminate operator dependence from the complete modelling process.

Once the centroidal representation has been generated, the bridge components are classified into independent AutoCAD layers according to their structural function. Dedicated layers are defined for longitudinal deck girders, pier shafts, pier caps, elastomeric bearings and auxiliary rigid links. This organization allows each category of structural elements to be systematically recognized during the DXF import procedure into MIDAS Civil, thereby reducing the need for manual reconstruction of structural entities within the FE environment. The layer-based organization also provides a standardized interface between the CAD and structural analysis environments.

Before exporting the DXF model, the continuity of the centroidal axes is verified at all deck–pier and deck–abutment connections to ensure nodal compatibility during the import into MIDAS Civil. This verification is intended to reduce connectivity inconsistencies during DXF import and the need for subsequent geometric corrections within the structural analysis environment. This step is particularly important for long multi-span bridges, where small geometric inconsistencies may generate connectivity errors during the automatic import procedure.

2.2. Finite Element Model Implementation

Once the CAD preprocessing has been completed, the DXF model is imported into MIDAS Civil [13], where each layer is automatically associated with the corresponding finite element typology. In particular, the bridge deck, piers and pier caps are discretized using beam elements. This modelling strategy provides a reduced-order representation intended to reproduce the main global characteristics required for seismic assessment while limiting the number of degrees of freedom. The influence of the adopted simplifications on the global structural response is discussed in Section 4. Unlike conventional finite element modelling procedures, where beams, supports and connectivity relationships are manually created inside the structural software, the proposed methodology directly transfers the structural topology from the CAD environment. Consequently, the finite element model is generated from the predefined CAD layers with limited user interaction during the model-transfer stage, reducing the need for manual reconstruction of structural entities within the FE environment. The layer-based organization also facilitates future updates of the numerical model. Modifications introduced in the CAD environment, such as changes in bridge geometry or support configuration, can be directly transferred to the finite element model through a new DXF import, avoiding extensive remodelling operations.

Elastomeric bearings are modelled by means of elastic links whose stiffness properties are calculated according to EN 1337-3 [14]. The interaction between beam elements and elastic links is ensured through rigid links, guaranteeing the correct transfer of forces between the superstructure and the substructure (Figures 1 and 2).

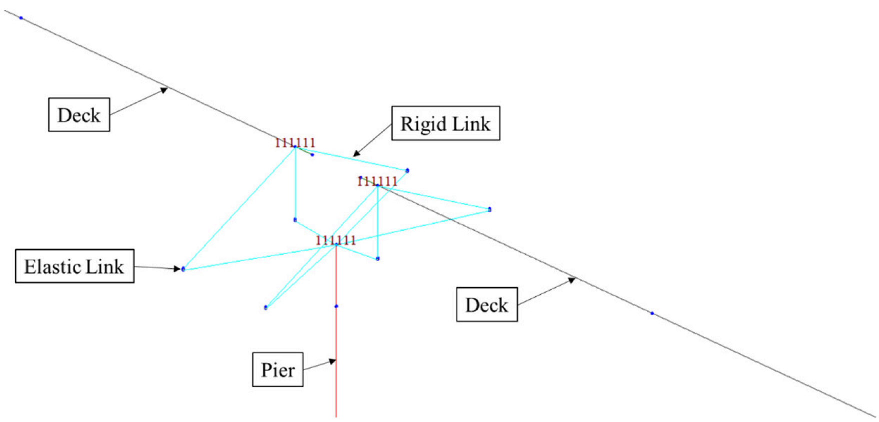

Figure 1. Layer-based centroidal representation adopted for CAD-to-FEM interoperability between AutoCAD and MIDAS Civil.

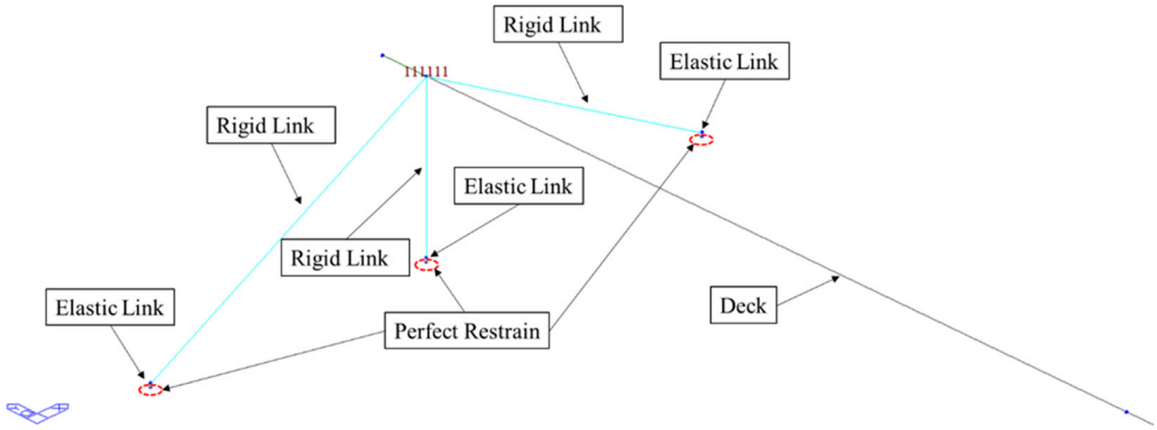

Figure 2. Detail of the simplified modelling strategy adopted for the deck–bearing–pier connection and abutment restraint.

The abutments are represented through fixed restraints applied to the base nodes of the elastic links, while the foundations of the piers are assumed fully restrained. These boundary-condition assumptions neglect foundation flexibility, soil–structure interaction, and possible nonlinear response of the abutment–soil system. Similarly, the elastic-link representation of the bearings does not account for potential nonlinear or degradation phenomena. These assumptions are adopted consistently with the global simplified modelling framework, but their influence on the dynamic and seismic response is not quantified in the present study.

The adopted modelling strategy is therefore intended as a simplified representation for global seismic assessment, with the limitations associated with the adopted modelling assumptions discussed in Section 4.

2.3. Material Constitutive Laws

The nonlinear behaviour of reinforced concrete is represented through the Kent and Park constitutive model for concrete [15] and the Park Strain Hardening model for reinforcing steel [16], shown in Figure 3.

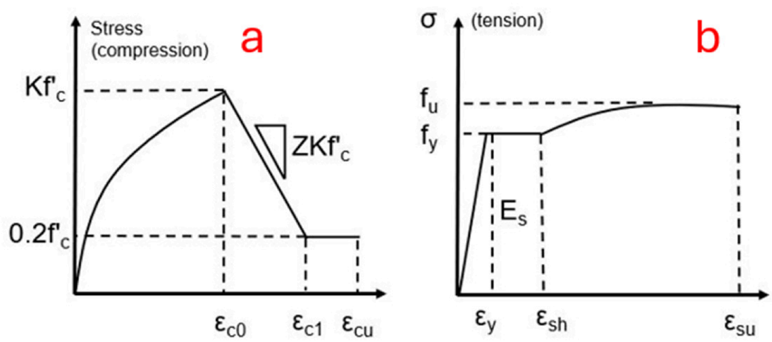

Figure 3. (**a**) Kent Park concrete model and (**b**) Park Strain Hardening constitutive law.

The mechanical properties adopted for the case study are summarized in Table 1. In particular, the bridge was designed using C28/35 concrete and FeB32K reinforcing steel. The actual material properties are determined according to the knowledge level achieved through the available investigations, consistent with the Italian Building Code [17]. When experimental information is unavailable, reference mechanical properties derived from previous technical studies are adopted [18].

Table 1. Materials mechanical properties.

C28/35	**f′$_c$** **[MPa]** 37.05	**Z** **[-]** 534	**K** **[-]** 1	**ε_{c0}** **[‰]** 2.00	**ε_{cu}** **[‰]** 3.50
FeB32K	**f_y** **[MPa]** 370	**f_u** **[MPa]** 433	**E_s** **[MPa]** 206,000	**ε_y** **[%]** 1.00	**ε_{su}** **[%]** 2.00

The reduction in the pier stiffness caused by concrete cracking is considered by applying a stiffness reduction coefficient derived from moment-curvature (M-χ) analyses, as suggested by Eurocode 8 [19].

2.4. Nonlinear Structural Assessment of the Generated FE Model

The seismic assessment described in this section is not part of the proposed CAD-to-FEM interoperability procedure itself. It is adopted as an application framework to demonstrate that the simplified FE model generated through the proposed workflow can be directly used for advanced seismic assessment. For this purpose, the established Multi-Modal Pushover Analysis (MPA) procedure is employed to account for the contribution of multiple significant vibration modes and to evaluate both ductile and brittle failure mechanisms.

The nonlinear response of the bridge is represented by means of concentrated plastic hinges located at the critical sections of the piers. Considering that the bridge piers exhibit a cantilever structural behaviour, plastic hinges are introduced at the pier bases and, where required, at the cross-section transitions of variable-section piers. The adopted modelling strategy is illustrated in Figure 4.

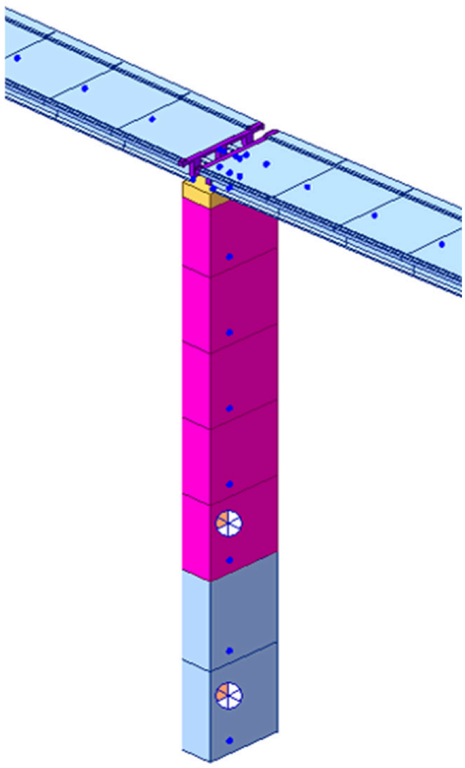

Figure 4. Plastic hinges applied to the piers.

The constitutive parameters defining each plastic hinge are derived from moment-curvature analyses of the corresponding cross-sections, while the idealized moment-rotation relationships are defined according to FEMA 356 [20]. Considering the Life Safety limit state, the verification criterion is taken equal to ¾ of the ultimate rotation ϑ_u.

Besides flexural behaviour, the numerical model also accounts for brittle shear failure. The shear resistance (V_R) of each pier is evaluated according to Equation (1):

$$V_R = \frac{1}{\gamma_{el}} \frac{h-x}{2L_V} \min(N; 0.55 A_c f_c) + \frac{1}{\gamma_{el}} \left(1 - 0.05 min\left(5; \mu_\Delta^{pl}\right)\right) \cdot \left[0.16 max(0.5; 100\rho_{tot}) \cdot \left(1 - 0.16 min\left(5; \frac{L_V}{h}\right)\right) \cdot \sqrt{f_c} A_c + V_w\right] \quad (1)$$

obtained by the sum of three factors that depend on axial load, concrete strength, and transverse steel reinforcement and where γ_{el} is equal to 1.15 considering the primary seismic elements, x is the height of the compressed area, N is the axial load, $\mu_\Delta{}^{pl}$ is the ductility expressed in terms of rotation, A_c is the cross-section area, ρ_{tot} is the total ratio of longitudinal steel reinforcement, V_w is the contribution of the transverse steel reinforcement and L_v is the shear span calculated considering a cantilever behavior of the piers. For this failure mechanism an elastic–brittle force–displacement constitutive law is adopted and the verification criterion for the above-mentioned limit state is taken equal to the achievement of the shear strength (V_R).

The consideration of both ductile and brittle mechanisms allows the proposed workflow to identify the governing collapse mechanism of each pier during the seismic assessment.

The simplified finite element model generated through the proposed CAD-to-FEM workflow is finally employed for seismic vulnerability assessment using the Multi-Modal Pushover Analysis (MPA). Unlike conventional pushover procedures, the adopted methodology considers all vibration modes characterized by a participating mass greater than 1%, following the approach proposed by [21]. An independent pushover analysis is performed for each selected vibration mode, producing a corresponding capacity curve. The curves are subsequently transformed into the Acceleration–Displacement Response Spectrum (ADRS) domain, and the performance point associated with each modal response is determined using the Capacity Spectrum Method (CSM) [22].

At the corresponding performance points, the internal forces acting on the monitored structural members are extracted and combined through the Complete Quadratic Combination (CQC) rule, allowing the overall seismic demand to be evaluated while accounting for the contribution of all significant vibration modes.

The simplified finite element model generated through the proposed CAD-to-FEM workflow is subsequently employed for seismic vulnerability assessment using the Multi-Modal Pushover Analysis (MPA). The procedure extends conventional pushover analysis by explicitly considering the contribution of multiple vibration modes and is therefore particularly suitable for bridges whose seismic response cannot be adequately represented by a single dominant mode. The adopted MPA procedure is carried out through the following steps. First, an eigenvalue analysis is performed to determine the vibration modes, natural periods, mode shapes and participating mass ratios of the bridge. Following the approach proposed in [21], all vibration modes characterized by a participating mass greater than 1% are retained in the analysis. For each selected mode, an independent nonlinear static analysis is then performed using a lateral load pattern associated with the corresponding modal response. This results in a modal capacity curve describing the nonlinear structural response for each significant vibration mode. Each capacity curve is subsequently transformed into the Acceleration–Displacement Response Spectrum (ADRS) domain, where the corresponding performance point is determined through the Capacity Spectrum Method (CSM) [22]. At each modal performance point, the relevant structural response quantities and internal forces of the monitored members are extracted. Since the individual modal responses are obtained independently, their contributions are subsequently combined using the Complete Quadratic Combination (CQC) rule. This allows the global seismic demand to account for the simultaneous contribution of the significant vibration modes. The seismic capacity is determined through an iterative procedure in which the intensity of the design response spectrum is progressively increased and the MPA procedure is repeated until the first monitored structural element reaches the prescribed limit state. Two independent failure mechanisms are considered. For the ductile mechanism, the limit state is governed by the rotational capacity of the concentrated plastic hinges, whereas for the brittle mechanism it corresponds to the attainment of the shear resistance of the piers. The Peak Ground Acceleration associated with the first attainment of each limit state is identified as the corresponding collapse acceleration (PGA_C). Finally, following the provisions of the Italian Building Code (NTC 2018) [17], the seismic performance of the bridge is quantified through the Peak Ground Acceleration and Return Period-based seismic risk indices defined in Equations (2) and (3):

$$RI_{PGA} = \frac{PGA_C}{PGA_D} \tag{2}$$

$$RI_{TR} = \left(\frac{RP_C}{RP_D}\right)^{0.41} \tag{3}$$

where PGA_D and RP_D represent the design seismic demand for the bridge site in terms of design peak ground acceleration and related return period, respectively, while RP_C is the return period associated with the collapse acceleration PGA_C. Values equal to or greater than unity indicate that the required seismic safety level is satisfied, whereas values lower than unity indicate insufficient seismic performance. Separate risk indices are calculated for the ductile and brittle mechanisms, allowing the governing seismic failure mode to be identified.

It is important to highlight that the parameters governing the nonlinear response are not empirically calibrated within the proposed workflow. The flexural hinge properties are derived from section-specific moment-curvature analyses, while the corresponding moment-rotation relationships and acceptance criteria are defined according to established code-based procedures [20,22]. Similarly, the brittle response is governed by the code-based shear resistance formulation described above. Consequently, the seismic vulnerability assessment is performed using standardized mechanical and code-based parameters rather than user-defined fitting parameters. This choice limits parameter arbitrariness and promotes consistency in the adopted assessment procedure.

In combination with the proposed layer-based CAD-to-FEM workflow, this procedure provides a structured framework for generating simplified numerical models and subsequently employing them within nonlinear seismic assessment procedures.

3. Case Study

To demonstrate the applicability of the proposed layer-based CAD-to-FEM workflow, the methodology was applied to an existing reinforced concrete highway bridge located in Northern Italy. The structure consists of two independent carriageways, one for each traffic direction, each composed of a sequence of fifteen simply supported spans. The bridge follows a rectilinear alignment in both plan and elevation, making it representative of a large number of RC bridges constructed along the Italian motorway network during the 1960s and 1970s. It should be noted that the investigated structure is characterized by a rectilinear alignment and a repetitive multi-span configuration. Therefore, the present case study should be regarded as a proof-of-concept application aimed at demonstrating the feasibility and implementation of the proposed CAD-to-FEM workflow rather than as a demonstration of its universal applicability to different bridge typologies. The extension of the procedure to geometrically irregular or structurally more complex bridges requires further validation. Accordingly, the

MPA-based seismic assessment presented below is intended to demonstrate the applicability of the generated FE model within an established nonlinear analysis framework, rather than to introduce or validate the MPA methodology itself.

The overall finite element model generated through the proposed workflow is shown in Figure 5. The first and last spans have a length of 33.80 m, whereas the intermediate spans are 34.40 m long.

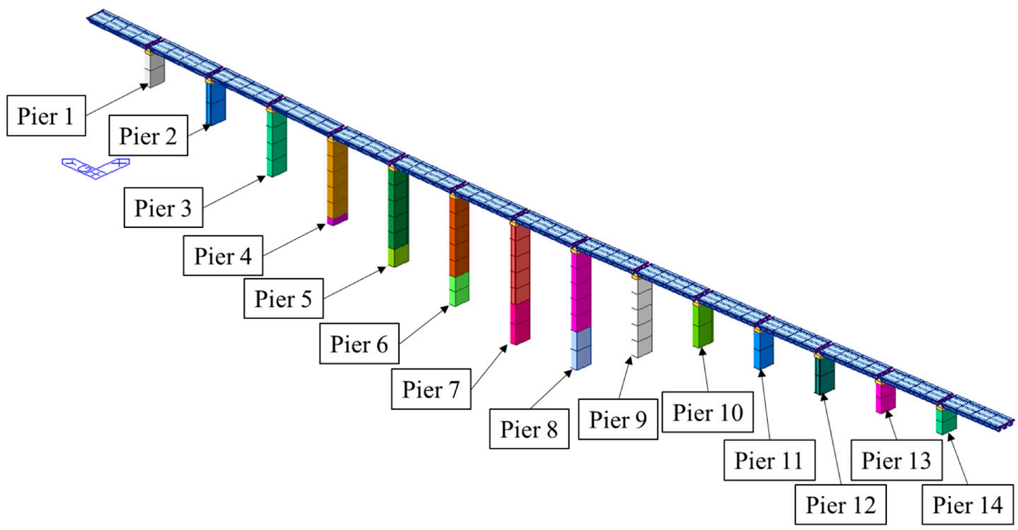

Figure 5. Beam-based finite element model generated through the proposed CAD-to-FEM workflow.

The deck has an overall width of 9.68 m (Figure 6) and consists of three longitudinal precast prestressed concrete I-girders connected by five transverse beams. Since the adopted modelling strategy is oriented toward a simplified global representation, the transverse beams are not explicitly discretized but are represented through equivalent nodal loads applied to the longitudinal girders. This approximation accounts for their contribution to the global mass distribution but does not explicitly reproduce their contribution to transverse deck stiffness and load redistribution. Consequently, its possible influence on the modal characteristics and transverse seismic response should be considered when interpreting the results.

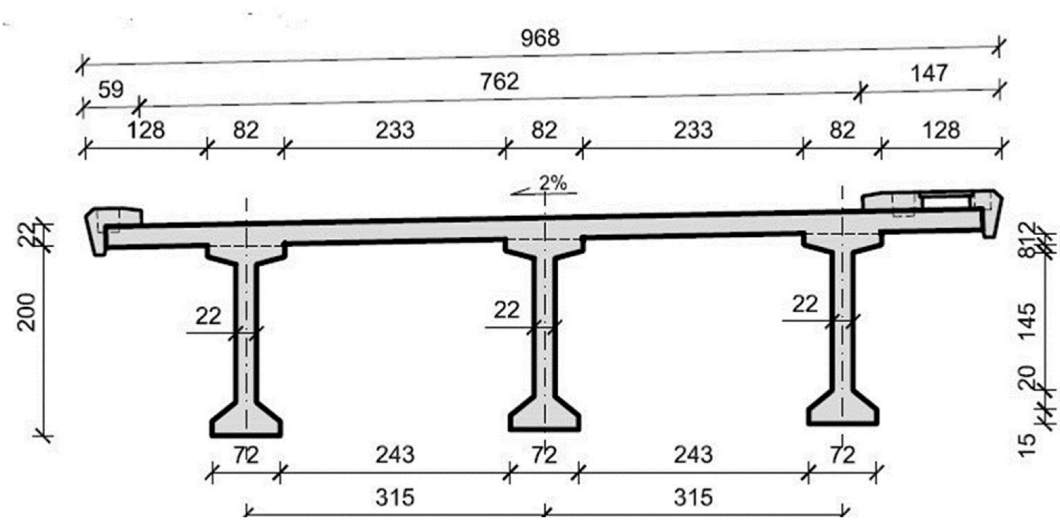

Figure 6. Section of the deck (u.m.: cm).

Each span is supported by nine rectangular elastomeric bearings arranged in a 3 × 3 configuration at both ends of the longitudinal girders. The geometric characteristics of the bearings adopted in the numerical model are reported in Figure 7.

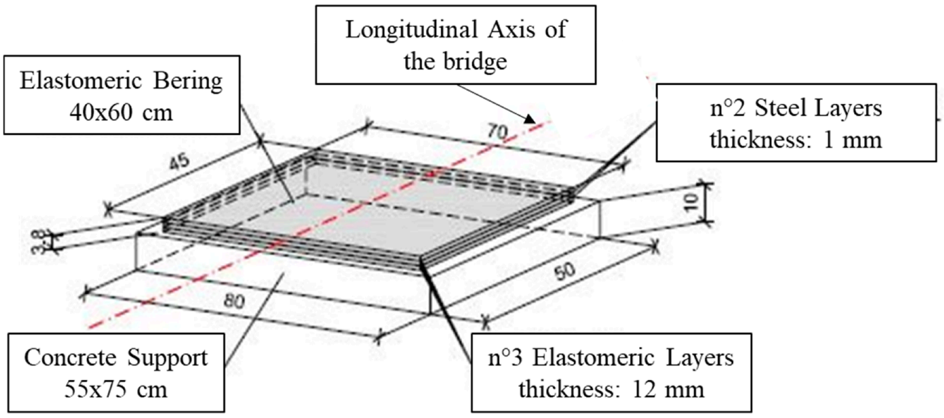

Figure 7. Elastomeric bearing (u.m.: cm).

The bridge substructure consists of hollow reinforced concrete piers having a rectangular cross-section measuring 8.00 × 3.30 m. Most piers have a constant wall thickness of 30 cm, whereas the central piers are characterized by a local increase in wall thickness to 45 cm in the lower portion in order to accommodate the larger axial loads. The main geometric and reinforcement characteristics of the bridge piers are summarized in Table 2.

Table 2. Main characteristics of the piers.

Pier	Height	Dimensions	Section Thickness	Longitudinal Rebars	Stirrups
[n°]	[m]	[m]	[m]	[-]	[-]
1	14.00	8.00 × 3.30	0.30	164Ø14	Ø10/20
2	18.50	8.00 × 3.30	0.30	164Ø14	Ø10/20
3	28.53	8.00 × 3.30	0.30	164Ø14	Ø10/20
4	3.00	8.00 × 3.30	0.45	164Ø20	Ø10/20
	34.00	8.00 × 3.30	0.30	164Ø14	Ø10/20
5	8.00	8.00 × 3.30	0.45	164Ø20	Ø10/20
	35.00	8.00 × 3.30	0.30	164Ø14	Ø10/20
6	13.00	8.00 × 3.30	0.45	164Ø20	Ø10/20
	35.00	8.00 × 3.30	0.30	164Ø14	Ø10/20
7	18.00	8.00 × 3.30	0.45	164Ø20	Ø10/20
	35.00	8.00 × 3.30	0.30	164Ø14	Ø10/20
8	16.97	8.00 × 3.30	0.45	164Ø20	Ø10/20
	35.00	8.00 × 3.30	0.30	164Ø14	Ø10/20
9	34.76	8.00 × 3.30	0.30	164Ø14	Ø10/20
10	18.46	8.00 × 3.30	0.30	164Ø14	Ø10/20
11	16.31	8.00 × 3.30	0.30	164Ø14	Ø10/20
12	15.98	8.00 × 3.30	0.30	164Ø14	Ø10/20
13	12.75	8.00 × 3.30	0.30	164Ø14	Ø10/20
14	10.46	8.00 × 3.30	0.30	164Ø14	Ø10/20

The investigated bridge is located in an area classified as having moderate-to-high seismic hazard according to [17]. The seismic input adopted throughout the study was defined according to the code provisions for the Life Safety Limit State (LSLS), considering the bridge importance class and the corresponding design reference life.

The design response spectrum was determined on the basis of the site seismic parameters summarized in Table 3, where V_N is the nominal service life, C_u is the importance coefficient, V is the reference life, P_{VR} is the probability of exceedance during the reference life, S_T is the topographic amplification coefficient, F_0 is the maximum amplification factor of the elastic response spectrum and T_C* is the characteristic period defining the constant-acceleration branch of the spectrum.

Table 3. Site parameters considered for the seismic assessment of the bridge.

Soil Type [-]	PGA [g]	V_N [Year]	Use Category [-]	C_u [-]	V [Year]	P_{VR} [%]	S_T [-]	F_0 [-]	T^*_C [s]
C	0.205	50	IV	2	100	10	1	2.47	0.305

The finite element model was generated by applying the workflow described in Section 2. The original engineering drawings of the bridge were first converted into a centroidal representation by replacing each structural member with its corresponding geometric axis. Subsequently, the bridge components were organized into dedicated AutoCAD layers according to their structural function, distinguishing deck members, pier shafts, pier caps, elastomeric bearings and auxiliary rigid links. The resulting DXF file was directly imported into MIDAS Civil, where each layer was automatically associated with the corresponding finite element typology. Beam elements were assigned to the deck and substructure members, whereas elastic links were adopted to represent the elastomeric bearings. The resulting finite element model is shown in Figure 5. Following the manual preparation and layer-based organization of the centroidal geometry in the CAD environment, the structural entities were transferred to MIDAS Civil through the DXF interface and associated with the corresponding finite element typologies. For the investigated bridge, this procedure provided a structured transition from the CAD representation to the analysis-ready numerical model. The present application therefore demonstrates the feasibility of the proposed interoperability procedure for a regular bridge characterized by a repetitive structural layout.

Following the generation of the numerical model through the proposed workflow, an eigenvalue analysis was carried out to identify the dynamic characteristics of the bridge. The participating mass ratios obtained for the significant vibration modes are summarized in Table 4 (where the x-axis corresponds to the longitudinal direction of the bridge, while the y-axis corresponds to the transverse direction), while the corresponding mode shapes are illustrated in Figure 8. As expected for long multi-span bridges, the dynamic response is governed by several vibration modes rather than by a single dominant mode. This behaviour confirms the necessity of adopting a Multi-Modal Pushover Analysis instead of a conventional pushover procedure.

The selected mode shapes shown in Figure 8 provide a qualitative representation of the principal deformation patterns governing the dynamic response of the bridge. The first vibration mode (T = 2.63 s) is predominantly associated with transverse motion, whereas the second mode (T = 1.84 s) primarily involves the longitudinal response. Higher modes introduce increasingly localized deformation patterns and contribute to the overall dynamic response, supporting the adoption of the Multi-Modal Pushover Analysis.

It should be emphasized that the mode shapes are normalized eigenvectors and that their graphical amplitudes are magnified only for visualization purposes. Consequently, the deformed configurations shown in Figure 8 do not represent actual seismic displacements, structural damage, or collapse conditions. Likewise, the graphical color variation is not associated with stress, damage, or limit-state utilization. Structural limit states are evaluated separately through the subsequent nonlinear analyses using the ductile and brittle verification criteria described in Section 2.4.

Table 4. Vibration modes.

Mode [n°]	Period (T) [s]	TRAN-X Mass [%]	TRAN-X Sum [%]	TRAN-Y Mass [%]	TRAN-Y Sum [%]
1	2.63	0.00	0.00	43.77	43.77
2	1.84	22.41	22.41	0.00	43.77
5	1.46	8.61	31.84	0.00	44.14
6	1.34	0.00	31.84	9.34	53.48
7	1.29	2.79	34.63	0.00	53.48
8	1.11	5.48	40.12	0.00	53.48
10	1.09	2.95	43.07	0.00	53.48
11	0.98	0.00	43.07	12.40	65.90
12	0.92	0.00	43.07	1.35	67.25
13	0.90	4.31	47.38	0.00	67.25
14	0.86	0.00	47.38	5.25	72.50
16	0.78	0.00	47.38	3.44	75.96
17	0.77	11.10	58.48	0.00	75.96
18	0.75	5.42	63.90	0.00	75.96
20	0.74	1.91	65.81	0.00	76.60
21	0.72	0.00	65.81	1.63	78.23
22	0.71	3.88	69.68	0.00	78.23
25	0.70	1.84	72.18	0.00	78.34
35	0.56	0.00	72.93	1.78	81.35
37	0.52	0.00	72.94	1.08	82.43
67	0.37	3.07	76.52	0.00	84.65
119	0.17	1.87	82.94	0.00	91.68
122	0.15	1.42	85.11	0.00	92.67

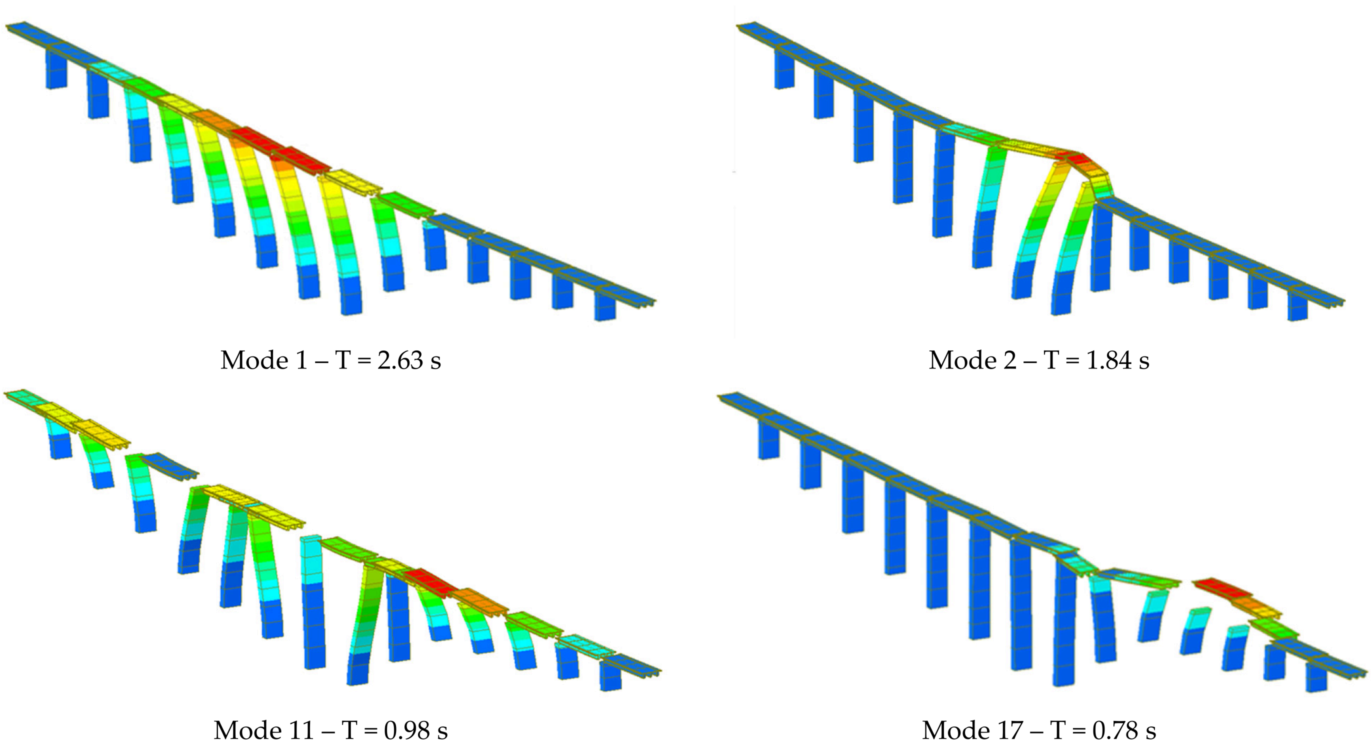

Figure 8. Selected normalized vibration mode shapes obtained from the linear eigenvalue analysis. (The displayed deformations are graphically amplified for visualization purposes and do not represent actual structural displacements or limit-state configurations.).

The moment-curvature relationships calculated for the representative piers are reported in Figure 9 and constitute the basis for defining the nonlinear moment-rotation constitutive laws adopted for the beam elements. The corresponding plastic hinge parameters are summarized in Table 5.

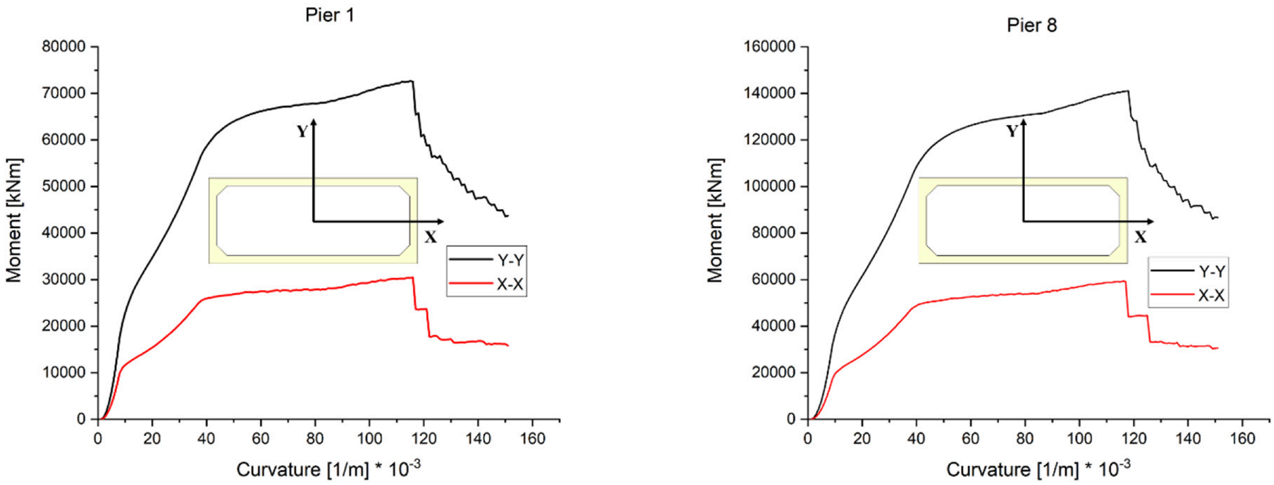

Figure 9. Moment-curvature diagram of the piers 1 (N = 8442 kN) and 8 (N = 16,261 kN).

Table 5. Moment-rotation plastic hinge law for piers 1 and 8.

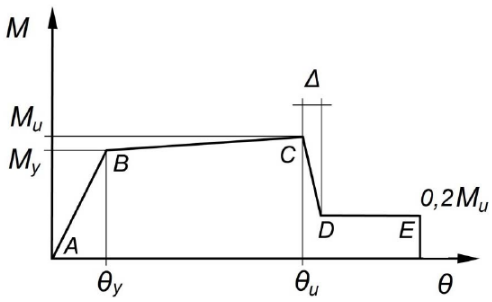

Pier	Section	Direction		A	B	C	D	E
1	Base	X-X	ϑ [rad]	0.000000	0.001521	0.015310	0.015325	0.016731
			M [kNm]	0.000000	25,065	30,479	6096	6096
		Y-Y	ϑ [rad]	0.000000	0.000858	0.008194	0.008202	0.008580
			M [kNm]	0.000000	56,478	72,291	14,458	14,458
8	Intermediate	X-X	ϑ [rad]	0.000000	0.002943	0.027340	0.027369	0.029430
			M [kNm]	0.000000	36,242	42,403	8481	8481
		Y-Y	ϑ [rad]	0.000000	0.001499	0.013827	0.013926	0.014990
			M [kNm]	0.000000	82,815	101,862	20,372	20,372
	Base	X-X	ϑ [rad]	0.000000	0.004053	0.038909	0.038949	0.040530
			M [kNm]	0.000000	47,338	59,172	11,834	11,834
		Y-Y	ϑ [rad]	0.000000	0.001946	0.018642	0.018662	0.019460
			M [kNm]	0.000000	105,632	140,490	28,098	28,098

The brittle behaviour was represented independently by calculating the shear resistance of each pier according to Equation (1). The resulting force–displacement relationships adopted for the brittle mechanism are reported in Table 6.

Table 6. Shear-displacement plastic hinge law for piers 1 and 8.

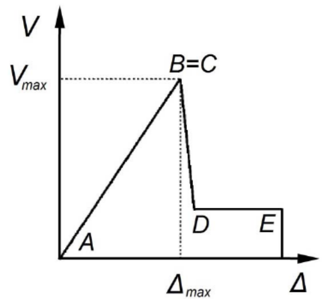

Pier	Section	Direction		Diagram Point A	B	C	D	E
1	Base	X	Δ [mm]	0.000000	0.2117	0.2117	0.2286	0.8468
			V [kN]	0.000000	4181	4182	836	836
		Y	Δ [mm]	0.000000	0.1629	0.1629	0.1759	0.6516
			V [kN]	0.000000	2002	2002	400	400
8	Intermediate	X	Δ [mm]	0.000000	0.3455	0.3455	0.3731	1.3820
			V [kN]	0.000000	3985	3985	797	797
		Y	Δ [mm]	0.000000	0.2814	0.2814	0.3039	1.1256
			V [kN]	0.000000	1782	1782	356	356
	Base	X	Δ [mm]	0.000000	0.2770	0.2770	0.2992	1.1080
			V [kN]	0.000000	3564	3564	713	713
		Y	Δ [mm]	0.000000	0.2509	0.2509	0.2709	1.0036
			V [kN]	0.000000	1744	1744	349	349

The Multi-Modal Pushover Analysis was then performed considering all vibration modes characterized by a participating mass greater than 1%. Examples of the capacity curves obtained for the ductile collapse mechanism are shown in Figure 10, whereas the corresponding curves for the brittle mechanism are reported in Figure 11.

For each vibration mode, the performance point was evaluated in the ADRS domain and the corresponding internal forces were extracted and combined using the Complete Quadratic Combination (CQC) rule. The iterative procedure described in Section 2 allowed the collapse acceleration and the corresponding seismic risk indices to be determined.

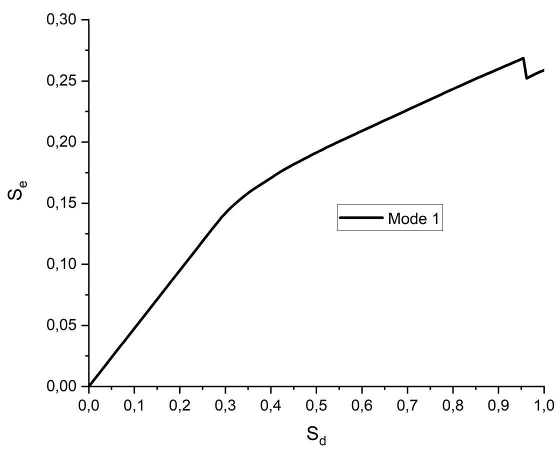

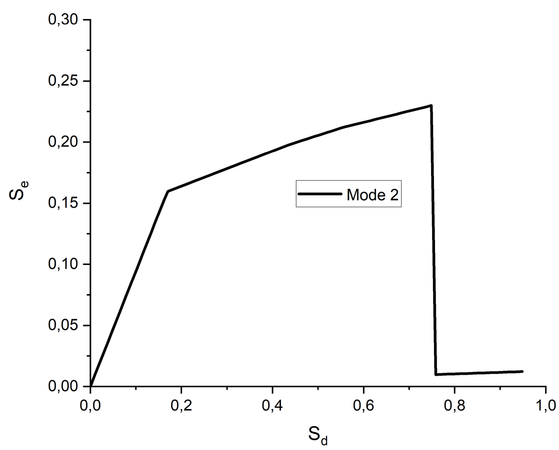

Figure 10. *Cont.*

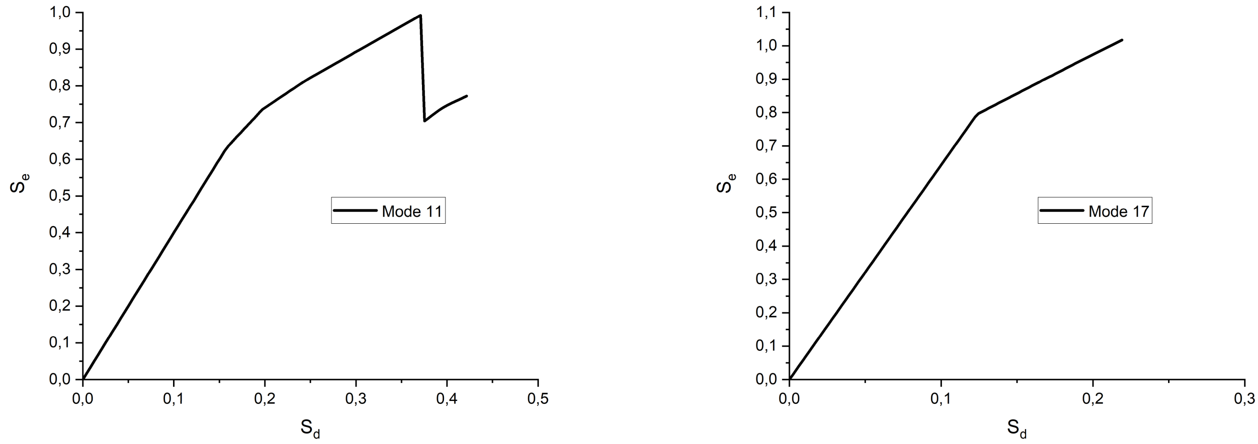

Figure 10. Capacity curves for ductile mechanism.

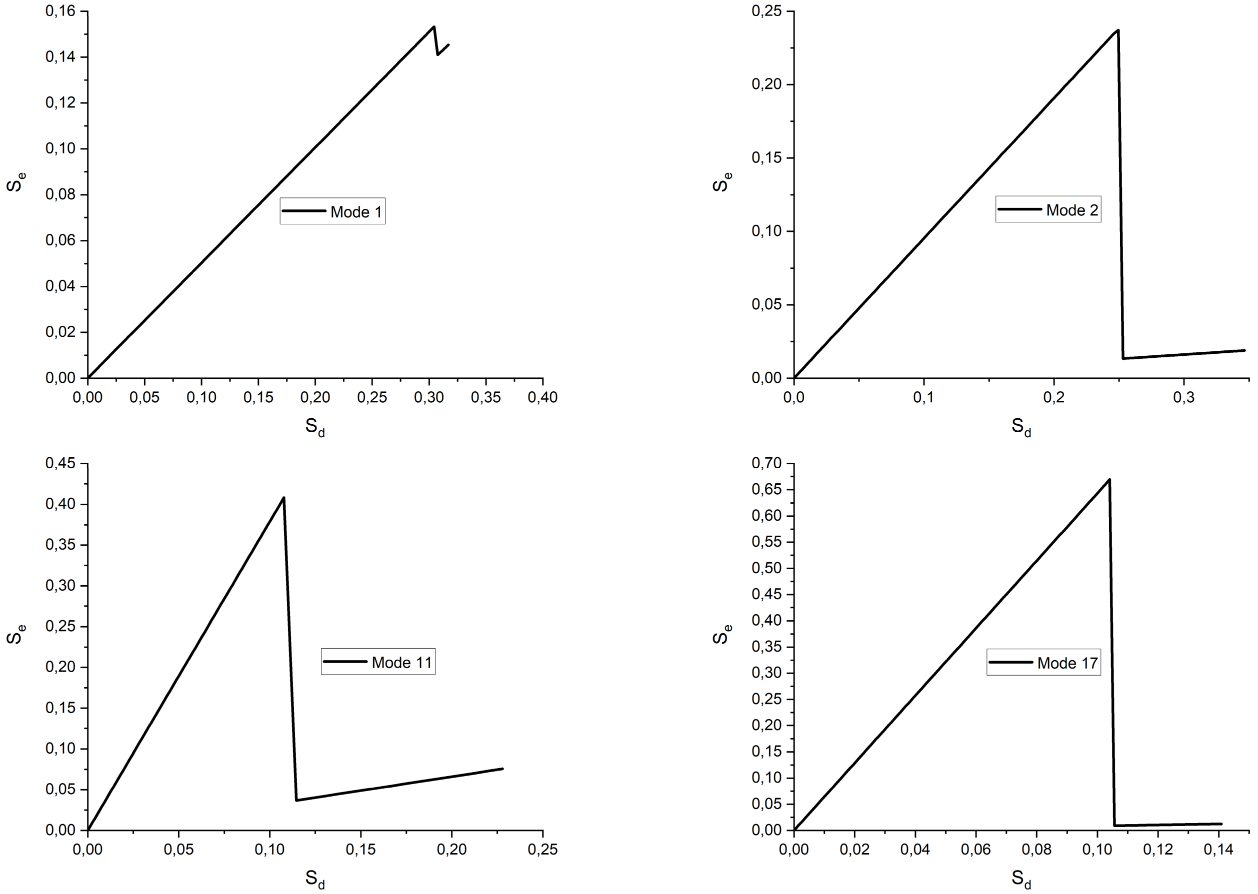

Figure 11. Capacity curves for brittle mechanism.

The final values of the seismic risk indices are reported in Tables 7 and 8.

Table 7. Risk indices obtained for ductile mechanism.

	X	Y
PGA_C [g]	0.664	0.770
RP_C [year]	19,855.64	29,062.12
RI_{PGA}	3.273	3.797
RI_{TR}	3.479	4.067

Table 8. Risk indices obtained for brittle mechanism.

	X	Y
PGA_C [g]	0.223	0.197
RP_C [year]	1211.08	886.48
RI_{PGA}	1.100	0.972
RI_{TR}	1.105	0.972

The results indicate that the bridge satisfies the required safety level with respect to the ductile mechanism in both principal directions, whereas the brittle mechanism governs the seismic vulnerability in the transverse direction due to the limited transverse reinforcement typical of bridges designed before the introduction of modern seismic provisions.

4. Discussion

The proposed CAD-to-FEM workflow demonstrates that the numerical modelling phase of existing reinforced concrete bridges can be standardized through a structured CAD preprocessing procedure. Unlike conventional modelling strategies, where the finite element model is manually generated within the analysis software, the proposed approach transfers the structural topology directly from the CAD environment by exploiting a layer-based organization of the bridge components. This considerably reduces user interaction during model generation while improving modelling consistency and interoperability. Furthermore, because the workflow relies exclusively on standard CAD entities and DXF interoperability, it can be implemented without requiring proprietary data exchange formats or customized software tools.

One of the main advantages of the proposed workflow is the clear separation between geometric modelling and structural analysis. The bridge geometry is prepared entirely within the CAD environment, where each structural component is represented by its centroidal axis and assigned to a dedicated layer. This organization enables direct interoperability with MIDAS Civil through the DXF format, considerably simplifying the generation of the finite element model and reducing the amount of manual editing normally required after import. Such an organization reduces the number of user-defined operations required during the CAD-to-FE transfer stage and provides a more standardized modelling sequence. However, because the initial structural interpretation and centroidal representation remain analyst-dependent, improved repeatability should be regarded as a potential benefit of the workflow rather than as a quantitatively demonstrated outcome of the present study. The standardized layer-based organization may also provide a basis for extending the workflow to the assessment of larger bridge inventories. However, this potential scalability has not been demonstrated in the present study, which considers only a single regular bridge typology. Its applicability to network-level assessment therefore requires further validation through systematic applications to bridges characterized by different geometries and structural configurations.

For the investigated bridge, the adopted beam-based representation provided an efficient modelling framework for the global seismic assessment. Since the objective of the study is the evaluation of the overall structural response rather than the local stress distribution, the simplified numerical model is intended to reproduce the principal global characteristics of the bridge while maintaining a limited number of degrees of freedom. Consequently, the limited number of degrees of freedom makes the adopted representation computationally suitable for nonlinear global analyses. However, its computational advantages in the context of large bridge inventories should be quantitatively assessed through applications to a broader range of bridge typologies.

The MPA-based case study serves as a proof-of-concept demonstration that the FE model generated through the proposed CAD-to-FEM workflow can be directly employed within an established nonlinear seismic assessment framework. The modal analysis confirms that the investigated bridge is characterized by several significant vibration modes, justifying the adoption of the Multi-Modal Pushover Analysis instead of conventional single-mode procedures. The calculated seismic risk indices show that the bridge exhibits satisfactory performance with respect to the ductile collapse mechanism, whereas the brittle shear mechanism governs the seismic vulnerability in the transverse direction. These results emphasize the importance of explicitly considering multiple failure mechanisms when evaluating existing reinforced concrete bridges.

The obtained results should also be considered in relation to current developments in seismic bridge assessment and digital structural modelling. Advanced nonlinear dynamic and fragility-based approaches can provide a more detailed characterization of seismic response and uncertainty, but their application generally requires substantial modelling and computational effort. Conversely, simplified nonlinear static procedures are particularly attractive when the objective is the systematic assessment of large bridge inventories, provided that the structural model adequately reproduces the global response and the relevant failure mechanisms. In this context, the present results confirm the importance of retaining higher-mode contributions for long multi-span bridges: the modal analysis identified several modes with significant participating mass, while the MPA procedure allowed their contributions to be incorporated into the seismic assessment.

From a digital modelling perspective, recent developments increasingly focus on detailed BIM models, point-cloud reconstruction and digital-twin environments. These approaches provide a high level of geometric and information detail, but such detail is not always required for global seismic assessment and may increase preprocessing effort before structural analysis. The proposed workflow follows a different but complementary strategy, retaining only the geometric and mechanical information required to generate a simplified analysis-ready model. Its main practical contribution is therefore not an increase in geometric fidelity, but a reduction and standardization of the modelling operations connecting conventional engineering drawings to nonlinear seismic analysis.

The case-study results also highlight the importance of distinguishing between modelling efficiency and structural-analysis accuracy. The simplified representation substantially facilitates model generation, whereas the seismic assessment itself retains the nonlinear features required to distinguish between ductile and brittle mechanisms. In the investigated bridge, the ductile mechanism satisfies the considered seismic demand, while the brittle shear mechanism governs the vulnerability in the transverse direction. This result is consistent with the broader observation that simplified global models can remain effective for preliminary and network-level seismic assessment only when potentially governing brittle mechanisms are explicitly considered rather than inferred solely from flexural response.

Despite these advantages, the proposed methodology presents limitations that define the current scope of its applicability. First, the workflow has been demonstrated on a single regular multi-span RC bridge characterized by a rectilinear alignment and a repetitive structural layout. Consequently, the present results demonstrate the feasibility of the proposed procedure but cannot establish its universal applicability to the broader range of existing bridge typologies. Further applications to bridges with curved alignments, skewed configurations, irregular geometries and different structural systems are required to assess the generality of the proposed approach. Moreover, the present study does not include a quantitative benchmark against an independently developed conventional finite element model. Therefore, the case study should be interpreted as a proof of concept demonstrating the feasibility of the proposed workflow rather than as a formal validation of its modelling accuracy or efficiency. A comprehensive validation should compare the generated and reference models in terms of structural mass and stiffness, modal periods and mode shapes, participating mass ratios, nonlinear capacity curves, internal force distributions, and resulting seismic risk indices. The adopted model also includes specific assumptions whose influence has not been independently quantified. In particular, replacing the transverse deck beams with equivalent nodal loads preserves their contribution to mass but neglects their explicit contribution to transverse stiffness and load redistribution. Furthermore, fully restrained pier foundations and abutments neglect foundation flexibility and soil–structure interaction, while the elastic-link representation of the bearings does not reproduce possible nonlinear or degradation effects. These assumptions may affect modal properties, internal force distributions and the resulting seismic response. Their influence should therefore be quantified in future studies through sensitivity analyses and comparison with more detailed reference models. Second, the simplified beam-based representation is intended for global structural assessment and cannot capture local three-dimensional stress concentrations, detailed joint behaviour or localized damage mechanisms. The current workflow should therefore be considered applicable primarily to bridges whose global structural behaviour can be adequately represented through beam elements and concentrated nonlinearities. More complex bridge typologies, such as cable-supported bridges or structures with steel orthotropic decks, may require additional modelling strategies or hybrid finite element formulations.

Future developments will focus on extending the interoperability procedure to Building Information Modelling (BIM) environments and point-cloud-based geometric reconstruction obtained from laser scanning or photogrammetric surveys. The integration of automated geometric recognition techniques with the proposed layer-based workflow could further reduce modelling time and facilitate the development of digital twins for the continuous monitoring and seismic assessment of existing bridge networks. Future work should include systematic benchmarking against independently developed reference FE models and inter-analyst comparisons to quantify modelling accuracy, analyst time, number of manual operations, preprocessing effort, total model-generation time, and repeatability across different bridge typologies.

Finally, the proposed workflow is currently semi-automatic because the centroidal representation must still be generated by the analyst within the CAD environment. Although the layer-based organization is intended to reduce subsequent manual model-generation operations, this benefit has not been quantitatively benchmarked against conventional FE modelling in the present study. Future developments should therefore focus on both the automatic extraction of centroidal axes from engineering drawings or point-cloud data and the quantitative evaluation of modelling efficiency.

5. Conclusions

This paper proposed a layer-based CAD-to-FEM workflow for the structured generation of simplified finite element models of existing RC bridges. The methodology combines centroidal geometric modelling, layer-based organization of structural components and direct DXF interoperability with MIDAS Civil, providing a standardized procedure for numerical model generation.

The proposed workflow was demonstrated through a proof-of-concept application in which the generated FE model was subsequently employed within an established Multi-Modal Pushover Analysis framework. The MPA was adopted as an application tool to verify the usability of the generated model for nonlinear seismic assessment and does not represent a methodological contribution of the present study. The generated beam-based model provided an analysis-ready representation of the bridge that enabled the evaluation of both ductile and brittle seismic collapse mechanisms through code-based risk indices.

The layer-based organization is intended to reduce user-dependent operations during model generation and to provide a more standardized transfer of structural information between the CAD and FE environments. These characteristics indicate the potential of the workflow to support infrastructure owners and engineering practitioners in the systematic assessment of bridge inventories, although its scalability to different bridge typologies remains to be demonstrated. Nevertheless, the repeatability of the complete modelling process has not been quantitatively assessed, since the initial interpretation of the drawings and generation of the centroidal representation still require analyst judgement.

The proposed CAD-to-FEM workflow represents an effective framework for integrating conventional engineering drawings with advanced nonlinear seismic analyses and provides a solid basis for future developments towards increasingly automated digital assessment procedures.

The application to the investigated bridge demonstrates the feasibility of integrating the proposed layer-based CAD-to-FEM workflow with advanced nonlinear seismic assessment procedures. The results support the potential of standardized CAD-to-FEM interoperability for the systematic generation of simplified structural models from conventional engineering drawings. However, the present study does not demonstrate scalability to large or heterogeneous bridge inventories. Further applications to bridges with different geometries, structural configurations and modelling requirements are necessary to assess the robustness, generality and scalability of the proposed approach.

From a practical perspective, the proposed methodology provides a structured procedure for transferring conventional bridge drawings into simplified FE models, while its efficiency for large bridge inventories remains to be quantitatively demonstrated.

Author Contributions: Conceptualization, M.Z., E.P. and P.C.; methodology, M.Z., P.C.; software, M.Z. and E.P.; validation, P.C.; formal analysis, M.Z.; investigation, P.C.; writing—original draft preparation, M.Z. and E.P.; writing—review and editing, P.C. All authors have read and agreed to the published version of the manuscript.

Funding: This research received no external funding.

Institutional Review Board Statement: Not applicable.

Informed Consent Statement: Not applicable.

Data Availability Statement: The original contributions presented in this study are included in the article. Further inquiries can be directed to the corresponding author.

Conflicts of Interest: The authors declare no conflicts of interest.

References

1. Reale, S.; Furinghetti, M.; Pavese, A. Numerical and experimental assessment of the seismic vulnerability of an existing bridge in presence of carbonation-induced corrosion. *Soil Dyn. Earthq. Eng.* **2026**, *200*, 109877. [CrossRef]
2. Serdar, N.N.; Pejovic, J.; Folic, R. Seismic Vulnerability of Curved RC Bridges Based on Displacement Ductility: Quantification and Curvature Effects. *J. Earthq. Eng.* **2026**, 1–27. [CrossRef]
3. Asen, F.; Pahlavan, H.; Amiri, M.S.; Naseri, A. Seismic fragility and vulnerability assessment of skew-curved box-girder bridges subjected to near- and far-fault earthquakes using dual intensity measures. *Structures* **2026**, *85*, 111142. [CrossRef]
4. Deng, L.; Wang, W.; Yu, Y. State-of-the-Art review on the causes and mechanisms of bridge collapse. *J. Perform. Constr. Facil.* **2016**, *30*, 04015005. [CrossRef]
5. d'Aragona, M.G.; Recupero, A.; Prota, A. Impact of corrosion on the lateral load response of RC multi-column bents with flex-ure-shear critical members. *Procedia Struct. Integr.* **2026**, *78*, 968–975. [CrossRef]
6. Crespi, P.; Zucca, M.; Longarini, N.; Giordano, N. Seismic assessment of six typologies of existing RC bridges. *Infrastructures* **2020**, *5*, 52. [CrossRef]

7. Paraskeva, T.S.; Kappos, A.J.; Sextos, A.G. Extension of modal pushover analysis to seismic assessment of bridges. *Earthq. Eng. Struct. Dyn.* **2006**, *35*, 1269–1293. [CrossRef]
8. Crespi, P.; Zucca, M.; Valente, M. On the collapse evaluation of existing RC bridges exposed to corrosion under horizontal loads. *Eng. Fail. Anal.* **2020**, *116*, 104727. [CrossRef]
9. Stefanidou, S.; Kappos, A.J. Methodology for the development of bridge-specific fragility curves. *Earthq. Eng. Struct. Dyn.* **2017**, *46*, 73–93. [CrossRef]
10. Chopra, A.K.; Goel, R.K. A modal pushover analysis procedure to estimate seismic demands for unsymmetric-plan buildings. *Earthq. Eng. Struct. Dyn.* **2004**, *33*, 903–927. [CrossRef]
11. Paraskeva, T.S.; Kappos, A.J. Further development of a multimodal pushover analysis procedure for seismic assessment of bridges. *Earthq. Eng. Struct. Dyn.* **2009**, *39*, 211–222. [CrossRef]
12. AutoCAD. Autodesk. 2025. Available online: https://www.autodesk.com/ (accessed on 3 August 2026).
13. Midas Civil. Analysis Reference. 2025. Available online: https://www.midasuser.com/en/product/civil (accessed on 3 August 2026).
14. *EN 1337-3:2005*; Structural Bearings–Part 3: Elastomeric Bearings. CEN (European Committee for Standardization). Management Centre: Brussels, Belgium, 2005.
15. Kent, D.C.; Park, R. Flexural members with confined concrete. *J. Struct. Div.* **1971**, *97*, 1969–1990. [CrossRef]
16. Park, R.; Paulay, T. *Reinforced Concrete Structures*; John Wiley and Sons: New York, NY, USA, 1973.
17. Ministerial Decree. *(NTC2018), Updating of Technical Codes for Constructions (in Italian), Official Gazette n.42 of 20/01/2018, Ordinary Supplement n.8*; Official Gazette: Rome, Italy, 2018.
18. Rossi, P.P.; Spinella, N.; Recupero, A. Experimental application of the Italian guidelines for the risk classification and management and for the safety evaluation of existing bridges. *Structures* **2023**, *58*, 105387. [CrossRef]
19. *EN 1998-2:2005*; Eurocode 8: Design of Structures for Earthquake Resistance–Part 2: Bridges. CEN (European Committee for Standardization). Management Centre: Brussels, Belgium, 2005.
20. Federal Emergency Management Agency. *Prestandard and Commentary for the Seismic Rehabilitation of Buildings*; FEMA 356; Federal Emergency Management Agency: Washington, DC, USA, 2000.
21. Chopra, A.K.; Goel, R.K. A modal pushover procedure to estimate seismic demands of buildings. *Earthq. Eng. Struct. Dyn.* **2002**, *31*, 561–582. [CrossRef]
22. *ATC-40:1996*; Seismic Evaluation and Retrofitting of Concrete Buildings. 8.1-8.66; Applied Technology Council: Redwood City, CA, USA, 1996.

https://doi.org/10.3390/app16178723